

3-乙基-2-乙酰吡嗪缩 4-甲基氨基硫脲 Ni(II)/Zn(II) 配合物的合成、结构和 DNA 结合性质

王碗碗 王 元* 于亚平 宋雨飞 吴伟娜*

(河南理工大学化学化工学院, 河南省煤炭绿色转化重点实验室, 焦作 454000)

摘要: 合成并通过单晶衍射、元素分析、红外光谱表征了配合物 $[\text{NiL}(\text{HL})](\text{OAc})$ (**1**) 和 $[\text{ZnL}(\text{OAc})]_n$ (**2**) 的结构 (HL=3-乙基-2-乙酰吡嗪缩 4-甲基氨基硫脲)。单晶衍射结果表明, 配合物 **1** 中的 Ni(II) 离子与来自 2 个缩氨基硫脲配体的 4 个 N 原子和 2 个 S 原子配位, 其中一个配体为阴离子。而配合物 **2** 中, 五配位的 Zn(II) 离子采取扭曲的四方锥配位构型, 与 2 个 μ -OCO 桥联的醋酸根, 一个三齿配位的缩氨基硫脲阴离子配位, 形成沿 a 轴方向的一维链状结构。此外, 荧光光谱结果表明, 配合物与 DNA 的相互作用强于配体。

关键词: 吡嗪; 缩氨基硫脲; 配合物; 晶体结构; DNA 结合性质

中图分类号: O614.81⁺3; O614.24⁺1

文献标识码: A

文章编号: 1001-4861(2018)08-1511-06

DOI: 10.11862/CJIC.2018.196

Ni(II)/Zn(II) Complexes with 1-(3-Ethylpyrazin-2-yl)ethylidene)-4-methylthiosemicarbazide: Crystal Structures and DNA-Binding Properties

WANG Wan-Wan WANG Yuan* YU Ya-Ping SONG Yu-Fei WU Wei-Na*

(College of Chemistry and Chemical Engineering, Henan Key Laboratory of Coal
Green Conversion, Henan Polytechnic University, Jiaozuo, Henan 454000, China)

Abstract: Two complexes $[\text{NiL}(\text{HL})](\text{OAc})$ (**1**) and $[\text{ZnL}(\text{OAc})]_n$ (**2**) (HL=1-(3-ethylpyrazin-2-yl)ethylidene)-4-methylthiosemicarbazide) have been synthesized and structurally determined by single-crystal X-ray diffraction. The results show that the Ni(II) ion in **1** is surrounded by two independent thiosemicarbazone ligands with N_4S_2 donor set, one of which is anionic. However, in complex **2**, the Zn(II) ion with a distorted tetragonal pyramid coordination geometry is five-coordinated, involving two μ -OCO acetate anions, one tridentate enolized ligand L^- , thus forming one dimension chain-like framework along a axis. Moreover, the fluorescence spectra indicate that the interactions of the complexes with DNA are stronger than that of the thiosemicarbazone ligand. CCDC: 1587278, **1**; 1587280, **2**.

Keywords: pyrazine; thiosemicarbazone; complex; crystal structure; DNA-binding property

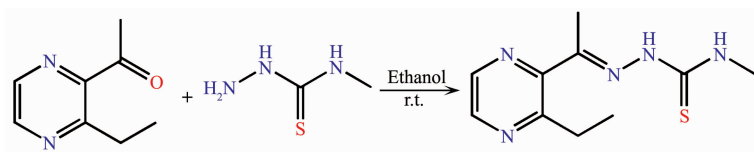
Thiosemicarbazones (TSCs) and their transition metal complexes have attracted intensity attention in the coordination chemistry because of their high biological and pharmaceutical activities^[1-4]. In most cases, metal-ligand synergism could occur (especially

Fe(III), Co(III), Ni(II), Cu(II), Zn(II) and Cd(II))^[5-7], although the mechanism of antitumor action is controversial in many respects and has been identified including ribonucleotide reductase inhibition^[8-9], metal dependent radical damage^[10], DNA binding^[11] and inhibition of

收稿日期: 2017-12-29。收修改稿日期: 2018-06-12。

国家自然科学基金(No.21001040)和河南省自然科学基金(No.182300410183, 162300410011)资助项目。

*通信联系人。E-mail: wangyuan08@hpu.edu.cn, wuwn08@hpu.edu.cn; 会员登记号: S06N6704M1112(吴伟娜)。



Scheme 1 Synthesis route of the TSC ligand HL

protein synthesis^[12].

As one of the most promising systems, the transition metal complexes of TSCs derived from 2-acetylpyridine/2-acetylpyrazine with different N(4)-substituents have been extensively studied as potential anticancer agents^[13-15]. To the best of our knowledge, however, the investigations on the complexes of TSCs derived from substituted 2-acetylpyrazine are relatively scarce^[14-15]. Taking into account this background and while searching for bioactive compounds, two complexes, namely $[\text{NiL}(\text{HL})](\text{OAc})$ (**1**) and $[\text{ZnL}(\text{OAc})]_n$ (**2**) (HL=1-(3-ethylpyrazin-2-yl)ethylidene-4-methylthiosemicarbazide) were synthesized and characterized by X-ray diffraction methods. In addition, DNA-binding properties of three compounds have been investigated in detail.

1 Experimental

1.1 Materials and measurements

Solvents and starting materials for syntheses were purchased commercially and used as received. Elemental analyses were carried out on an Elemental Vario EL analyzer. The IR spectra ($\nu=4\,000\sim 400\text{ cm}^{-1}$) were determined by the KBr pressed disc method on a Bruker V70 FT-IR spectrophotometer. DNA-binding properties of both complexes are measured using literature method via emission spectra^[16]. The UV spectra were recorded on a Purkinje General TU-1800 spectrophotometer. Fluorescence spectra were determined on a Varian CARY Eclipse spectrophotometer, in the measurements of emission and excitation spectra the pass width was 5 nm.

1.2 Syntheses of HL, complexes **1** and **2**

A mixture of 3-ethyl-2-acetylpyrazine (1.50 g, 10 mmol) and N(4)-methylthiosemicarbazide (1.05 g, 10 mmol) in ethanol (30 mL) were stirred for 4 h at room temperature. The white solid HL precipitated, then was filtered and washed three times by cold ethanol.

Yield: 1.87 g (79%). m.p. 137.0~137.9 °C. Elemental analysis Calcd. for $\text{C}_{10}\text{H}_{15}\text{N}_5\text{S}$ (%): C 50.61; H 6.37; N 29.51; Found(%): C 50.79; H 6.22; N 29.74. ^1H NMR (400 MHz, CDCl_3): δ 8.78 (1H, s, NH), 8.53~8.54 (2H, t, pyrazine-H), 3.25~3.36 (3H, d, CH_3), 3.11~3.15 (2H, q, $\text{CH}_2\text{-CH}_3$), 2.39 (3H, s, CH_3), 1.35~1.37 (3H, t, $\text{CH}_3\text{-CH}_2$). FT-IR (cm^{-1}): $\nu(\text{N}=\text{C})$ 1 544, $\nu(\text{N}=\text{C}, \text{pyrazine})$ 1 502, $\nu(\text{S}=\text{C})$ 863.

Complex **1** was synthesized by reacting HL (0.5 mmol) with $\text{Ni}(\text{OAc})_2$ (ligand-metal molar ratio 2:1) in methanol (20 mL) solution at room temperature. The block crystals suitable for X-ray diffraction analysis were obtained by evaporating the reaction solutions at room temperature. Complex **2** is prepared by the same procedure, while using $\text{Zn}(\text{OAc})_2$ instead of $\text{Ni}(\text{OAc})_2$.

1: Brown blocks. Yield: 58%. Anal. Calcd. for $\text{C}_{22}\text{H}_{32}\text{N}_{10}\text{O}_2\text{S}_2\text{Ni}$ (%): C, 44.68; H, 5.45; N, 23.68. Found (%): C, 44.57; H, 5.58; N, 23.58. FT-IR (cm^{-1}): $\nu(\text{N}=\text{C})$ 1 534, $\nu(\text{N}=\text{C}, \text{pyrazine})$ 1 474, $\nu_a(\text{COO})$ 1 569, $\nu_s(\text{COO})$ 1 420, $\nu(\text{S}=\text{C})$ 821.

2: Yellow blocks. Yield: 62%. Anal. Calcd. for $\text{C}_{12}\text{H}_{17}\text{N}_5\text{O}_2\text{SZn}$ (%): C, 39.95; H, 4.75; N, 19.41. Found (%): C, 40.15; H, 4.83; N, 19.23. FT-IR (cm^{-1}): $\nu(\text{N}=\text{C})$ 1 527, $\nu(\text{N}=\text{C}, \text{pyrazine})$ 1 477, $\nu_a(\text{COO})$ 1 584, $\nu_s(\text{COO})$ 1 413, $\nu(\text{S}=\text{C})$ 822.

1.3 X-ray crystallography

The X-ray diffraction measurement for complexes **1** (Size: 0.20 mm×0.18 mm×0.16 mm) and **2** (Size: 0.16 mm×0.15 mm×0.03 mm) was performed on a Bruker SMART APEX II CCD diffractometer equipped with a graphite monochromatized Mo $K\alpha$ radiation ($\lambda=0.071\,073\text{ nm}$) by using $\varphi\text{-}\omega$ scan mode. Semi-empirical absorption correction was applied to the intensity data using the SADABS program^[17]. The structures were solved by direct methods and refined by full matrix least-square on F^2 using the SHELXTL-97 program^[18]. The C6 atom of **1** occupied two positions, with the occupancy value of C6/C6A being 0.358/

0.642. All non-hydrogen atoms were refined anisotropically. All H atoms were positioned geometrically and refined using a riding model. Details of the

crystal parameters, data collection and refinements for complexes **1** and **2** are summarized in Table 1.

CCDC: 1587278, **1**; 1587280, **2**.

Table 1 Crystal data and structure refinement for complexes **1** and **2**

	1	2
Empirical formula	C ₂₂ H ₃₂ N ₁₀ O ₂ S ₂ Ni	C ₁₂ H ₁₇ N ₅ O ₂ SZn
Formula weight	590.40	360.73
<i>T</i> / K	296(2)	296(2)
Crystal system	Monoclinic	Monoclinic
Space group	<i>P</i> 2 ₁ / <i>c</i>	<i>P</i> 2 ₁ / <i>c</i>
<i>a</i> / nm	0.877 27(12)	0.913 1(6)
<i>b</i> / nm	1.346 91(18)	1.599 7(11)
<i>c</i> / nm	2.315 0(3)	2.173 9(14)
β / (°)	100.337(3)	91.777(13)
<i>V</i> / nm ³	2.691 0(6)	3.174(4)
<i>Z</i>	4	8
<i>D_c</i> / (g·cm ⁻³)	1.460	1.517
<i>F</i> (000)	1 240	1 488
Data, restraint, parameter	4 737, 3, 352	5 553, 27, 387
Goodness-of-fit (GOF) on <i>F</i> ²	1.014	1.059
Final <i>R</i> indices [<i>I</i> > 2σ(<i>I</i>)]	<i>R</i> ₁ =0.050 0, <i>wR</i> ₂ =0.072 7	<i>R</i> ₁ =0.043 7, <i>wR</i> ₂ =0.090 6
<i>R</i> indices (all data)	<i>R</i> ₁ =0.110 4, <i>wR</i> ₂ =0.086 4	<i>R</i> ₁ =0.076 6, <i>wR</i> ₂ =0.101 9

2 Results and discussion

2.1 Crystal structures description

The diamond drawings of complexes **1** and **2** are

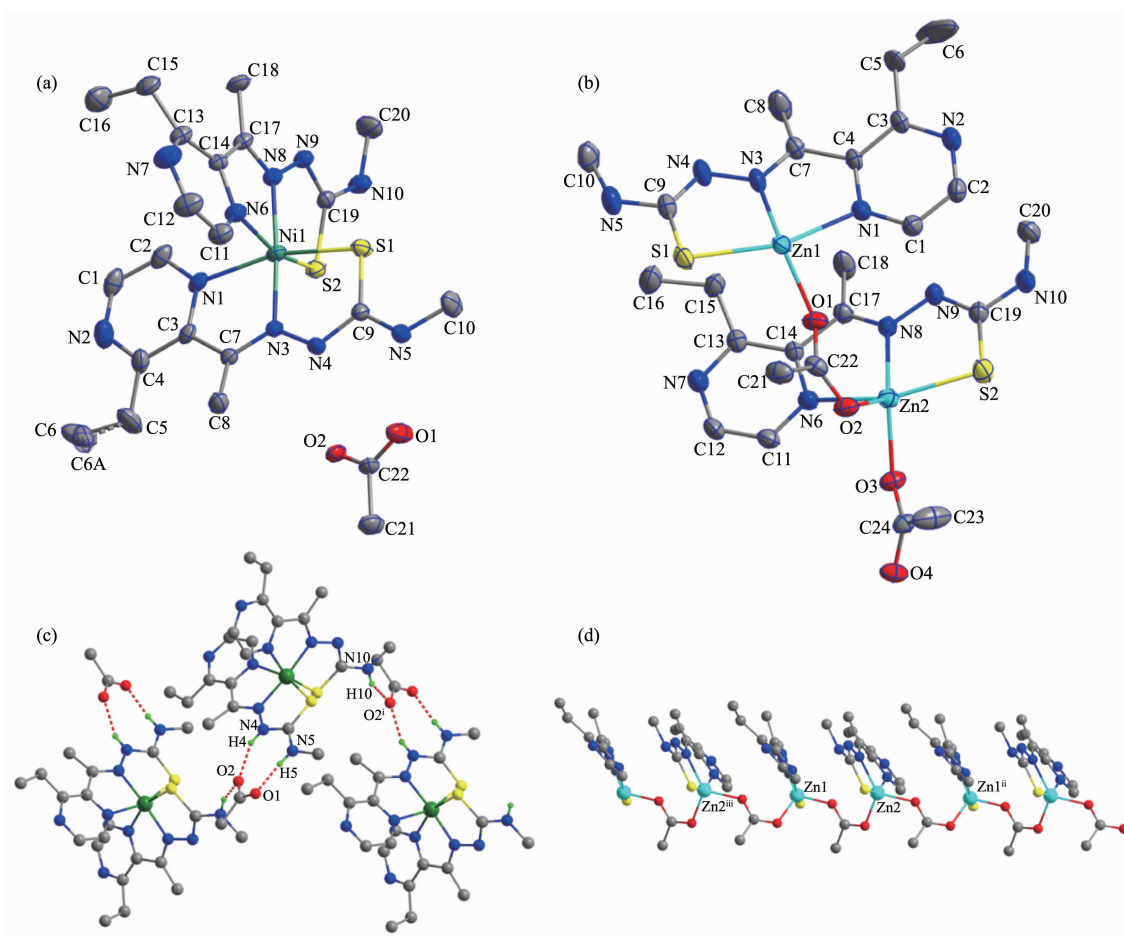
shown in Fig.1. Selected bond distances and angles are listed in Table 2. As shown in Fig.1a, the asymmetric unit of complex **1** contains a coordination cation and a free acetate anion for charge balance.

Table 2 Selected bond lengths (nm) and angles(°) in complexes **1** and **2**

1					
Ni1-N1	0.211 4(3)	Ni1-N3	0.201 2(3)	Ni1-S1	0.238 66(12)
Ni1-N6	0.210 3(3)	Ni1-N8	0.199 3(3)	Ni1-S2	0.239 85(12)
N8-Ni1-N3	174.11(14)	N6-Ni1-N1	85.25(13)	N8-Ni1-S2	82.50(10)
N8-Ni1-N6	77.00(14)	N8-Ni1-S1	98.21(9)	N3-Ni1-S2	103.10(9)
N3-Ni1-N6	97.28(13)	N3-Ni1-S1	83.25(10)	N6-Ni1-S2	159.11(10)
N8-Ni1-N1	101.03(13)	N6-Ni1-S1	91.96(9)	N1-Ni1-S2	94.87(9)
N3-Ni1-N1	76.87(13)	N1-Ni1-S1	159.39(10)	S1-Ni1-S2	94.91(4)
2					
Zn1-O1	0.201 9(3)	Zn1-O4 ⁱⁱⁱ	0.199 5(3)	Zn1-N1	0.222 3(3)
Zn1-N3	0.211 7(3)	Zn1-S1	0.233 77(19)	Zn2-O2	0.200 6(3)
Zn2-O3	0.202 9(3)	Zn2-N6	0.220 8(3)	Zn2-N8	0.211 1(3)
Zn2-S2	0.235 5(19)				
O4 ⁱⁱⁱ -Zn1-S1	110.84(9)	O4 ⁱⁱⁱ -Zn1-N1	89.49(12)	O4 ⁱⁱⁱ -Zn1-O1	97.79(12)
O1-Zn1-S1	105.50(9)	O1-Zn1-N1	86.26(12)	O4 ⁱⁱⁱ -Zn1-N3	126.46(13)

Continued Table 2

N3-Zn1-S1	81.92(9)	N3-Zn1-N1	73.18(12)	O1-Zn1-N3	129.76(12)
N1-Zn1-S1	154.31(10)	O2-Zn2-S2	111.72(10)	O2-Zn2-N6	91.53(13)
O2-Zn2-O3	97.53(12)	O3-Zn2-S2	105.09(9)	O3-Zn2-N6	84.00(12)
O2-Zn2-N8	126.15(13)	N8-Zn2-S2	82.27(10)	N8-Zn2-N6	72.91(13)
O3-Zn2-N8	129.95(12)	N6-Zn2-S2	153.16(9)		

Symmetry codes: ⁱⁱⁱ 1+x, y, zHydrogen bonds shown in dashed line; Symmetry codes: ⁱ -x, -0.5+y, 0.5-z; ⁱⁱ -1+x, y, z; ⁱⁱⁱ 1+x, y, zFig.1 ORTEP drawing of **1** (a) and **2** (b) with 30% thermal ellipsoids; (c) Chain-like structure along *a* axis formed via N-H \cdots O hydrogen bonds in complex **1**; (d) 1D chain like structure along *a* axis in complex **2**

The center Ni(II) ion is coordinated by two TSC ligands with N₄S₂ donor sets, and thus possesses a distorted octahedron coordination geometry. It should be noted that one of the TSC ligands is neutral with C-S bond length (C9-S1) being 0.168 4(4) nm, which is similar as that of the reported TSCs^[19], while quite shorter than that of its counterpart (C19-S2, 0.173 2(4) nm). The distances of Ni-N/S bonds were in the range of 0.199 3(3)~0.2398 5(12) nm, which were comparable with those found in the reported complexes with similar

donor set^[14-15]. In the crystal, free acetate anions link the complex cations via intermolecular N-H \cdots O hydrogen bonds (N4-H4 \cdots O2ⁱ, with D \cdots A distance being 0.270 7(4) nm, D-H \cdots A angle being 148.4°; N5-H5 \cdots O1, with D \cdots A distance being 0.267 1(5) nm, D-H \cdots A angle being 172.0°; N10-H10 \cdots O2ⁱⁱ, with D \cdots A distance being 0.297 1(4) nm, D-H \cdots A angle being 148.7°, Symmetry code: ⁱ -x, -0.5+y, 0.5-z) into one-dimensional chains along *a* axis (Fig.1c).

There exist two independent Zn(II) ions with

similar coordination environment in the asymmetric unit of complex **2** (Fig.1b). Each Zn(II) ion is five-coordinated, involving two μ -OCO acetate anions, one tridentate enolized ligand L^- , thus forming one dimension chain-like framework along a axis (Fig.1d). According to the Addison rule^[20], the geometric index τ is 0.414 and 0.391 for Zn1 and Zn2, respectively, indicating that the coordination geometry of each Zn(II) ion is best described as a distorted tetragonal pyramid rather than trigonal bipyramid. However, no classical hydrogen bonds are presented in the structure of **2**.

2.2 IR spectra

The infrared spectral bands most useful for determining the coordination mode of the ligand are the $\nu(N=C)$, $\nu(N=C, \text{ pyrazine})$ and $\nu(S=C)$ vibrations. Such three bonds of the free TSC ligand is found at 1 544, 1 502 and 863 cm^{-1} , while they shifts to lower frequency in complexes **1** and **2**, clearly indicating the coordination of imine nitrogen, pyrazine nitrogen and sulfur atoms^[14-15]. In addition, the general pattern of the IR spectroscopy supports the existence of free and μ -OCO acetate groups in complexes **1** and **2**, respectively^[21]. It is in accordance with the X-ray diffraction analysis result.

2.3 UV spectra

The UV spectra of HL, complexes **1** and **2** in CH_3OH solution (concentration: 10 $\mu\text{mol} \cdot \text{L}^{-1}$) were measured at room temperature (Fig.2). The spectra of HL features only one main band located around 299 nm ($\epsilon=34\,026 \text{ L} \cdot \text{mol}^{-1} \cdot \text{cm}^{-1}$), which could be assigned

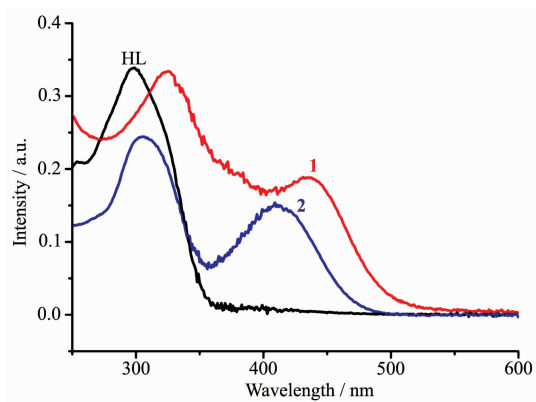
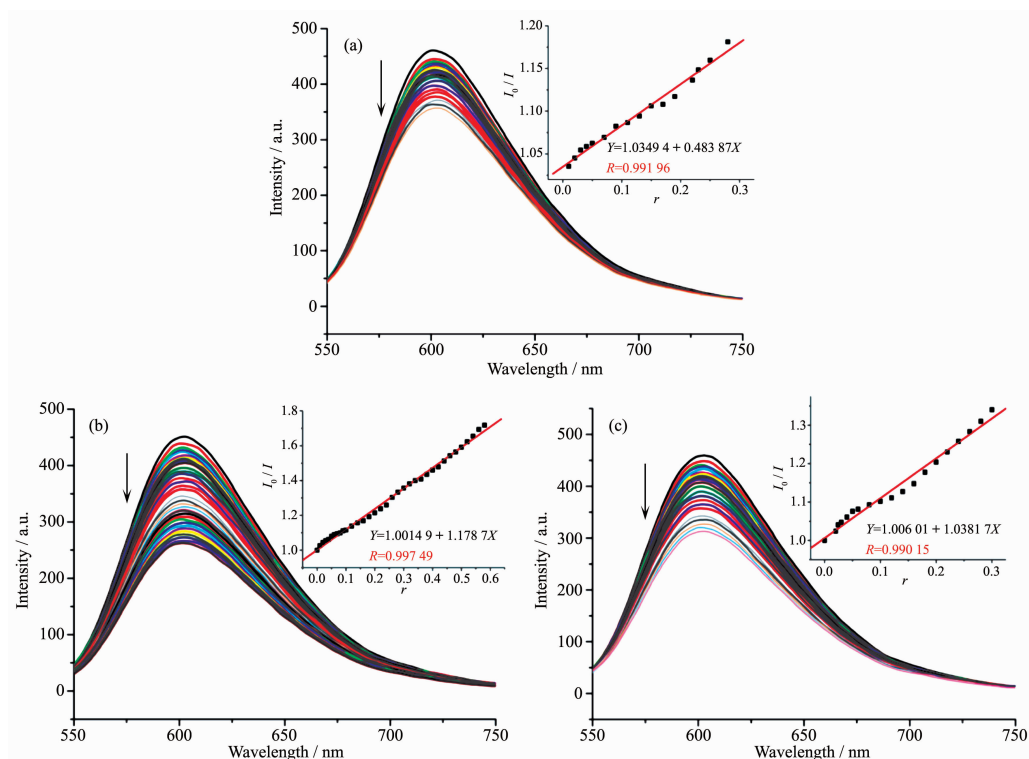


Fig.2 UV spectra of the ligand HL, **1** and **2** in CH_3OH solution at room temperature

to characteristic $\pi-\pi^*$ transition of pyrazine unit^[16]. Similar bands are observed at 323 nm ($\epsilon=33\,725 \text{ L} \cdot \text{mol}^{-1} \cdot \text{cm}^{-1}$) and 304 nm ($\epsilon=24\,475 \text{ L} \cdot \text{mol}^{-1} \cdot \text{cm}^{-1}$) in the complexes **1** and **2**, respectively. However, the new bands at 435 nm ($\epsilon=19\,092 \text{ L} \cdot \text{mol}^{-1} \cdot \text{cm}^{-1}$) and 410 nm ($\epsilon=15\,240 \text{ L} \cdot \text{mol}^{-1} \cdot \text{cm}^{-1}$) could be observed in spectra of **1** and **2**, respectively, probably due to the ligand-to-metal charge transfer (LMCT)^[22]. This indicates that an extended conjugation is formed in anionic ligand after complexation in the complexes.

2.3 EB-DNA binding study by fluorescence spectrum

It is well known that EB can intercalate into DNA to induce strong fluorescence emission. Competitive binding of other drugs to DNA and EB will result in displacement of bound EB and a decrease in the fluorescence intensity^[16]. Fig.3 shows the effects of HL, complexes **1** and **2** on the fluorescence spectra of EB-DNA system. The fluorescence emission peak of EB bound to ct-DNA is at about 600 nm, which shows remarkable decreasing trend with the increasing concentration of each tested compound. This fact indicates that some EB molecules are released into solution after the exchange with the compound. The quenching of EB bound to DNA by the compound is in agreement with the linear Stern-Volmer equation: $I_0/I=1+K_{\text{sq}}r^{[21-22]}$, where I_0 and I represent the fluorescence intensities in the absence and presence of quencher, respectively; K_{sq} is the linear Stern-Volmer quenching constant; r is the ratio of the concentration of quencher and DNA. In the quenching plots of I_0/I versus r , K_{sq} values are given by the slopes. The K_{sq} values are 0.484, 1.179 and 1.038 for HL, complexes **1** and **2**, respectively, indicating that interaction of the complexes with DNA is stronger than HL. This is probably due to the structure rigidity and metal-ligand synergism effect of the complexes^[16]. Complex **1** has higher quenching ability than **2**, because **1** possesses zero dimensional structure while **2** has an infinite chain-like framework. In addition, the coordination environment of the metal ion may be also responsible for the DNA interaction ability in some extent.



Arrow shows the fluorescence intensities change of EB-DNA system upon increasing tested compound concentration; Inset: plot of I_0/I versus r

Fig.3 Emission spectra of EB-DNA system in the presence of HL (a), complexes **1** (b) and **2** (c)

References:

- [1] Ramachandran E, Raja D S, Rath N P, et al. *Inorg. Chem.*, **2013**,**52**:1504-1514
- [2] Ivanovic I, Gligorijevic N, Arandelovic S, et al. *Polyhedron*, **2013**,**61**:112-118
- [3] Almeida S M, Lafayette E A, Silva L P, et al. *Int. J. Mol. Sci.*, **2015**,**6**:13023-13042
- [4] Zhang X M, Guo H, Li Z S, et al. *Eur. J. Med. Chem.*, **2015**, **101**:419-430
- [5] Sangeetha K G, Aravindakshan K K. *Inorg. Chim. Acta*, **2018**, **469**:387-396
- [6] Milunovic M N M, Dobrova A, Novitchi G, et al. *Eur. J. Inorg. Chem.*, **2017**,**469**:4473-4483
- [7] Wang Y T, Fang Y, Zhao M, et al. *MedChemComm*, **2017**,**8** (11):2125-2132
- [8] Kowo C R, Trond R, Arion V B, et al. *Dalton Trans.*, **2010**, **39**:704-706
- [9] Zeglis B M, Divilov V, Lewis J S. *J. Med. Chem.*, **2011**,**54**: 2391-2394
- [10] Enyedy É A, Primik M F, Kowol C R, et al. *Dalton Trans.*, **2011**,**40**:5895-5905
- [11] Ramachandran E, Thomas S P, Poornima P, et al. *Eur. J. Med. Chem.*, **2012**,**50**:405-415
- [12] Raja D S, Paramaguru G, Bhuvanesh N S, et al. *Dalton Trans.*, **2011**,**4**:4548-4559
- [13] Al-Eisawi Z, Stefani C, Jansson P J, et al. *J. Med. Chem.*, **2016**,**59**:294-312
- [14] Li M X, Zhang L Z, Yang M, et al. *Bioorg. Med. Chem. Lett.*, **2012**,**22**:2418-2433
- [15] Li M X, Zhang L Z, Zhang D, et al. *Eur. J. Med. Chem.*, **2011**,**46**:4383-4390
- [16] LIN Long(林龙), LI Xian-Hong(李先宏), ZHANG Bo(张波), et al. *Chinese J. Inorg. Chem.*(无机化学学报), **2017**,**33**:143-148
- [17] Sheldrick G M. *SADABS*, University of Göttingen, Germany, **1996**.
- [18] Sheldrick G M. *SHELX-97, Program for the Solution and the Refinement of Crystal Structures*, University of Göttingen, Germany, **1997**.
- [19] LI Xiao-Jing(李晓静), MAO Pan-Dong(毛盼东), WU Wei-Na(吴伟娜), et al. *Chinese J. Inorg. Chem.*(无机化学学报), **2017**,**33**:1257-1265
- [20] Addison A W, Rao T N. *J. Chem. Soc. Dalton Trans.*, **1984**: 1349-1356
- [21] Nakamoto K. *Infrared and Raman Spectra of Inorganic and Coordination Compounds: Part B. 6th Ed.* New York: Wiley, **2009**:65
- [22] MAO Pan-Dong(毛盼东), ZHAO Xiao-Lei(赵晓雷), SHAO Zhi-Peng(邵志鹏), et al. *Chinese J. Inorg. Chem.*(无机化学学报), **2017**,**33**:890-896